

Combining Remote Sensing and Modeling for Estimating Surface Evaporation and Biomass Production

M. SUSAN MORAN

USDA-ARS U.S. Water Conservation Laboratory, 4331 E. Broadway, Phoenix, AZ 85040, USA

STEPHAN J. MAAS

USDA-ARS Cotton Research Station, 17503 N. Shafter Ave., Shafter, CA 93263, USA

PAUL J. PINTER, JR.

USDA-ARS U.S. Water Conservation Laboratory, 4331 E. Broadway, Phoenix, AZ 85040, USA

ABSTRACT

A simple approach for simulation of daily regional evaporation and plant primary production is proposed. The approach is based on an existing plant growth model combined with a simple soil water balance equation for simulation of evaporation rates. The resulting model was specifically designed to incorporate periodic remotely-sensed estimates of plant leaf area index (LAI) and daily surface evaporation (E). The model was evaluated based on spectral, meteorologic, agronomic and soils data acquired during a two-year experiment in an alfalfa stand at the U.S. Water Conservation Laboratory lysimeter field plots in Phoenix, Arizona. The remotely-sensed inputs to the model (LAI and E) were obtained from measurements of surface reflectance and temperature, combined with measurements of air temperature. Then, the model was used to simulate daily values of E, LAI and biomass production using infrequently-acquired remotely-sensed information and routinely available meteorologic observations. These results illustrated the potential for use of ground- and satellite-based spectral measurements as supplemental input for a simulation model to monitor, assess and forecast regional water and plant biomass resources.

INTRODUCTION

Remote sensing can be an effective means for estimating surface evaporation and plant canopy density over a geographic region (see reviews by Jackson (1985) and Moran and Jackson (1991)). While satellite-based sensors can easily be used to survey large areas on the earth's surface, a drawback to their use in operational monitoring programs is the relative infrequency of observations of a given loca-

tion as a result of overpass schedules and the occurrence of cloud cover. Thus, satellite-based observations represent discrete time events which may indicate little about the evolution of the biosystem to its observed state or indications of its condition in the future.

Numerous simulation models of the vegetation-soil-atmosphere system have been developed to provide continuous description of vegetation growth and evaporation. To be consistently accurate, these models generally require an extensive database of site-specific meteorologic and edaphic information (e.g., Sellers et al., 1986). The difficulty and expense of collecting this information on a regional scale often make the use of simulation models impractical for regional monitoring.

A possible solution to the operational monitoring problem is to use a simpler model which requires less ground information and supplement the model with periodic estimates of key input parameters. Such models have been successfully developed for agricultural crops to simulate plant growth (Maas, 1988a, 1988b, 1991a, 1991b), based on routinely available meteorologic observations such as average daily air temperature and total daily solar irradiance. Simulation accuracy was increased by "calibrating" model parameters with infrequent field observations of actual plant growth obtained during the growing season (Maas, 1993a, 1993b).

In the work presented here, we present two modifications to an existing plant growth simulation model that have potential to expand its application and increase its accuracy. First, we combined the plant growth model with a simple soil water balance equation to simulate both crop biomass production and evaporation. Second, we used remotely-sensed estimates of leaf area index (LAI) and evaporation (E) instead of direct field measurements for the simulation calibration procedure (Maas et al., 1992; Moran et al., 1992).

By its nature, such a model is dependent upon development of accurate methods for estimation of crop biomass and evaporation using remotely-sensed spectral data. On-going research in this area suggests that there is great potential for accurate estimation of such surface properties using remotely-sensed spectral data (see next section). The intent of this report is not to investigate such algorithms, but rather to assume that accurate estimates of LAI and E are possible, and to conduct a preliminary evaluation of the accuracy of the simulation model. Accordingly, we selected specific methods for evaluation of LAI and E and refined these for use in an alfalfa stand in Phoenix, AZ. Thus, we obtained a general estimate of the error associated with the model inputs of LAI and E. Then, using daily observations of meteorological data and periodic remotely-sensed estimates of LAI and E, a preliminary demonstration of the model was conducted to evaluate its performance.

REMOTE SENSING BACKGROUND

Satellite- and ground-based measurements of surface reflectance have been related to critical model requirements, such as land cover (Tucker, 1979) and vegetation status (Jackson et al., 1983). Furthermore, surface temperature and re-

flectance have been combined with ground-based meteorologic data to directly evaluate surface energy fluxes, such as net radiation and evaporation (Jackson et al., 1977). An elementary understanding of the theoretical and practical bases behind these relationships will facilitate further discussion.

Spectral Vegetation Indices for Discrimination of Vegetation Properties

Vegetation indices, based on reflectance in the visible and near-infrared (NIR) spectral bands, are commonly used to discriminate plant parameters such as biomass and leaf area index (Jackson and Huete, 1992). Due to the differential energy scattering properties of vegetation canopies, the simple ratio (SR) of the NIR reflectance (ρ_{NIR}) to red reflectance (ρ_{red}) has been reported to be a sensitive indicator of green biomass (Tucker, 1979), where

$$\text{SR} = \rho_{\text{NIR}} / \rho_{\text{red}}. \quad (1)$$

Though spectral vegetation indices such as SR are designed to be sensitive to vegetation characteristics, there is evidence that they are also responsive to such unrelated variables as solar zenith angle (Ranson and Daughtry, 1987) and, in the case of airborne and satellite-based sensors, atmospheric interference (Jackson et al., 1983). For temporal analysis of vegetation, these unrelated influences must be taken into account. In this analysis, the spectral data were acquired at ground level, thus eliminating the influence of atmospheric effects. Furthermore, the spectral data were acquired in mid-morning resulting in a solar zenith angle range over the growth cycle of only 5° . These precautions were necessary to minimize the significant influences of physical factors other than vegetation.

Remote Estimation of Daily Evaporation

An expression relating E to surface temperature minus air temperature ($T_s - T_a$) was developed by Jackson et al. (1977) based on a simplification of energy balance theory, where

$$E = R_n - G - (\rho c_p (T_s - T_a) / r_{ah}). \quad (2)$$

In Eq. (2), R_n is daily net radiation and G is daily soil heat flux density. The third term is an expression for sensible heat flux density, where ρc_p is the volumetric heat capacity of air and r_{ah} is a resistance to heat transfer. This resistance term can be expressed simply in terms of wind speed and surface roughness as

$$r_{ah} = (\{\ln[z/z_0]\}/k)^2 / u, \quad (3)$$

where z is the height above the surface where wind speed (u) is measured, z_0 is the aerodynamic roughness length, and k is von Karman's constant (Brutseart, 1982). In this expression, z_0 represents the height within the canopy where wind speed would be zero, if the wind speed were to decrease linearly with the logarithm of depth in the canopy. The value of z_0 is commonly estimated from plant height (h) based on empirical studies of the logarithmic wind profile over mature crop canopies (Monteith, 1973).

To use Eq. (2) in a practical situation, Jackson et al. (1977) suggested some simplifying assumptions. They concluded that for 24-hour periods, the soil heat flux density G was negligible. Based on their experimental data, they also assumed that $\rho c_p / r_{ah}$ remained constant, thus simplifying the equation to a linear form,

$$E = A + B(T_s - T_a), \quad (4)$$

where A and B are empirical coefficients.

The assumption that $\rho c_p / r_{ah}$ was constant in Eq. (2) was viable for the mature wheat crop studied by Jackson et al. (1977) for two reasons. First, they found that the r_{ah} value was not sensitive to wind speed within the range of wind speeds occurring during the experiment. Second, the height of the wheat crop did not vary substantially during the measurement period, resulting in a relatively constant value of z_0 . For crops of variable height and cover, such as the alfalfa stand studied in this experiment, the crop cover can vary from 0 to 100% for each growing period. Thus, Eq. (4) must necessarily be revised to include r_{ah} in order to encompass both immature and mature crop canopies, where

$$E = A' + B'(T_s - T_a) / r_{ah}, \quad (5)$$

and A' and B' are empirical coefficients.

The inclusion of the r_{ah} term in Eq. (5) appears to defeat the original intent of Jackson et al. (1977) to derive a simple empirical relation for estimation of E . However, the relation between z_0 and plant height (Monteith, 1973) provides the opportunity for a simple empirical evaluation of r_{ah} in Eq. (5). That is, assuming that z_0 is related to crop height, and assuming that surface reflectance is influenced in part by plant height (Moran, 1990), it follows that z_0 , and consequently r_{ah} , are likely related to spectral vegetation indices. Thus, the only information necessary to solve Eq. (5) would be values of T_s , T_a , ρ_{NIR} and ρ_{red} . This hypothesis was tested based on the ancillary micrometeorologic data acquired during this experiment.

The fundamental limitation on the application of Eqs. (4) and (5) is the dependence upon clear-sky conditions. Since these relations are used to determine the *daily* evaporation from *instantaneous* ($T_s - T_a$), values of A , B , A' and B' shouldn't be evaluated using data acquired when variable cloudy conditions influence the instantaneous rate of evaporation.

THE MODEL

The model consists of two submodels—a soil water balance submodel and a vegetation growth submodel. These submodels operate in sequence to produce simulations of evapotranspiration, soil moisture, leaf canopy density, and biomass production. A numerical procedure called within-season calibration is used in the model to manipulate the values of certain parameters and initial conditions so that model simulations are brought into agreement with remotely-sensed estimations.

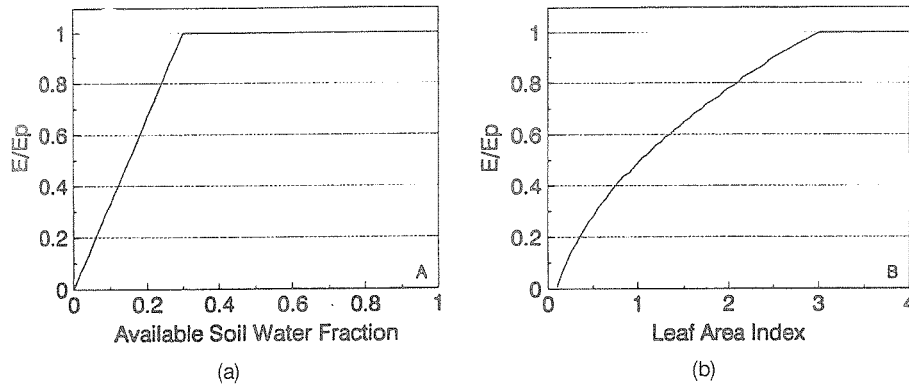


FIGURE 1 Relationship between the ratio E/E_p and (a) available soil water fraction (f_{sw}) [from Meyer and Green, 1980; Rosenthal et al., 1987] and (b) vegetation canopy leaf area index (LAI) [from Ritchie and Burnett, 1971].

Soil Water Balance Submodel

The formulation of the soil water balance submodel is based on the following assertions:

1. For vegetated surfaces in arid and semi-arid environments, the contribution of soil surface evaporation to evapotranspiration (E) is relatively small compared to the contribution from plant transpiration, except immediately after a rainfall; and
2. When soil water is abundant, E approaches potential E (E_p) for the vegetation canopy.

Based on these observations, one may conceptualize that, on any given day, regional E is determined by the degree to which the E of the vegetation canopy approaches E_p and the degree to which the vegetation canopy covers the region.

Studies involving agricultural crops (cf. Meyer and Green, 1980; Rosenthal et al., 1987) indicate that the ratio E/E_p appears to be a function of the available soil water fraction in the rooting zone (Figure 1(a)). Available soil water fraction (f_{sw}) is defined as the amount of soil water between the wilting point for the vegetation and the maximum drained capacity for the field, normalized by the maximum drained capacity. Maximum drained capacity is often called "field capacity".

Ritchie and Burnett (1971) showed that, when soil water was abundant, the ratio of vegetation transpiration to E_p could be expressed as a consistent function of LAI for dissimilar agricultural crops (cotton and grain sorghum). The form of this function is shown in Figure 1(b), where it has been assumed that vegetation canopy E is equivalent to vegetation transpiration.

Based on this information, daily E was computed in the soil water balance submodel using the following relationship,

$$E = E_p F_{sw} F_{GC} \quad (6)$$

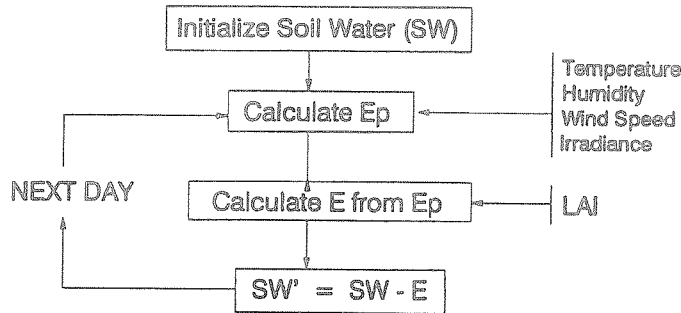


FIGURE 2 Sequence of steps in computing daily E_p , E and soil water (SW) in the soil water balance submodel.

in which F_{SW} is the ratio E/E_p from Figure 1(a) and F_{GC} is the ratio E/E_p from Figure 1(b). E_p was computed from routinely-available meteorologic observations (average daily air temperature, average daily dew point temperature, average daily wind speed and total daily solar irradiance) using the combination equation described and validated by Van Bavel (1966).

Changes in soil water and E were simulated with a daily time step using the stepwise process depicted in Figure 2. Daily values of LAI for evaluating F_{GC} were obtained from the vegetation growth submodel. Hydrologic processes such as rainfall, runoff and infiltration of water upward into the rooting zone were not explicitly incorporated into this initial version of the submodel. An initial amount of soil water was specified at the start of the simulation. With each storm or irrigation event, the soil moisture parameter was updated to account for the existing soil moisture and the amount of soil moisture added by rainfall.

Vegetation Growth Submodel

The formulation of the vegetation growth submodel is similar to that used in earlier agricultural crop growth models (Maas, 1992; Maas et al., 1989). Operating with a daily time step, the submodel simulated the change in aboveground vegetation biomass and LAI using the stepwise process depicted in Figure 3.

Photosynthetically active radiation (PAR) was assumed to comprise 45% of the total daily solar irradiance (Brown, 1969). PAR absorbed by the vegetation canopy (APAR) was computed using the relationship,

$$APAR = PAR[1 - e^{-k(LAI)}] \quad (7)$$

in which k is the extinction coefficient (Charles-Edwards et al., 1986). Production of new biomass (ΔB) was determined using the relationship,

$$\Delta B = APAR \epsilon f(T_a) \quad (8)$$

where the parameter ϵ is the "energy conversion efficiency" (Charles-Edwards et al., 1986) and $f(T_a)$ is a function that reduces the rate of biomass production at suboptimum air temperatures (T_a). New leaf area in the canopy is determined

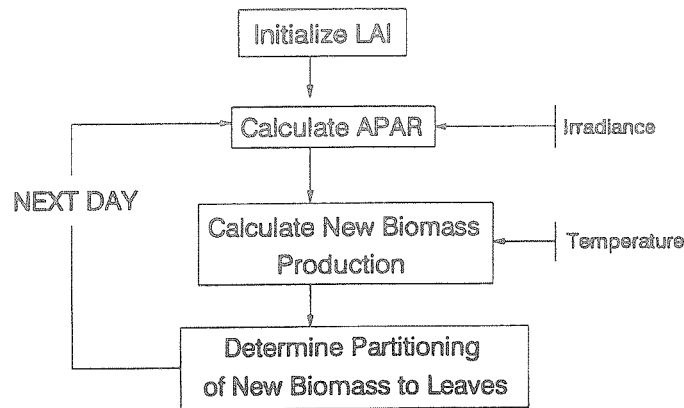


FIGURE 3 Sequence of steps in computing daily biomass growth and changes in canopy leaf area index in the vegetation growth submodel [from Maas, 1993a].

by partitioning a model-derived fraction of ΔB to leaf biomass and multiplying this quantity by the specific leaf area (i.e., the m^2 of leaf area per kg of leaf biomass) of the vegetation. On the day of its formation, new leaf area is assigned a lifespan in terms of accumulated degree-days that determines how long it will live prior to senescence from the vegetation canopy. The submodel maintains a running total of degree-days (computed from average daily air temperature) to determine what portion of the canopy leaf area is alive or dead on any given day of the simulation.

Within-Season Model Calibration

Remotely-sensed data are not required to simulate evapotranspiration and biomass production using this model. However, the consistent accuracy of this relatively simple model should be improved by the acquisition of infrequent estimates of E and LAI based on remotely sensed spectral measurements. Maas (1988a) showed that the most effective method of incorporating infrequent remotely-sensed information into plant growth models was through reinitialization and/or reparameterization. In these procedures, which are collectively termed "within-season calibration", the values of certain model initial conditions and/or parameters are manipulated until the model simulation of a quantity fits a corresponding set of remotely-sensed estimates. An iterative numerical procedure (Maas, 1993b) is built into the model to manipulate the initial conditions and/or parameters so that they converge on values that result in the model simulation fitting the set of remotely-sensed estimates (Figure 4). Although this numerical procedure is based solely on statistics, Maas (1991a, 1991b) demonstrated that within-season calibration could significantly improve the accuracy of agricultural crop growth models.

For this study, remotely-sensed estimates of E were used to calibrate the soil water balance submodel, while remotely-sensed estimates of LAI were used to calibrate the vegetation growth submodel. In the soil water balance submodel,

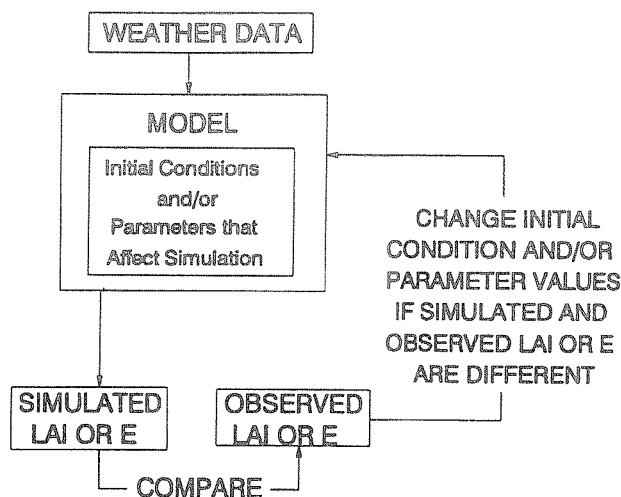


FIGURE 4 Diagrammatic representation of the within-season calibration procedure [from Maas, 1993b].

the initial value of soil water and the value of field capacity were manipulated to bring the E simulation into agreement with the corresponding observations. In the vegetation growth submodel, the initial value of LAI, the value of leaf life-span and the value of a parameter that controls the partitioning of new biomass to leaves were manipulated to bring the LAI simulation into agreement with the corresponding observations.

In simulating evapotranspiration and biomass production using this model, the vegetation growth submodel is accessed first and calibrated using the remotely-sensed LAI estimates. The resulting set of simulated daily LAI values is then used in an iteration of the soil water balance submodel, which is calibrated using the remotely-sensed E estimates.

EXPERIMENT

An alfalfa field at the U.S. Water Conservation Laboratory (USWCL), Phoenix, AZ, was the site for this research. Micrometeorologic data were monitored on a half-hour basis, and spectral and agronomic characteristics of the crop were observed on a regular basis (daily or weekly) over a two-year period. Results from this experiment have been reported by several authors (Pinter et al., 1987; Moran et al., 1990) and the following descriptions of the experimental materials and methods were excerpted from these publications.

Field Description and Preparation

An 80 × 60 m field was segmented into 18 plots separated by low beams of about 0.2 m height. Alfalfa seeds (*Medicago sativa* L. cv Lew) were broadcast at a rate

of 43.5 kg ha⁻¹. The soil was an Avondale loam [fine-loamy, mixed (calcareous), hyperthermic Anthropic Torrifluvent]. After one year's growth, a differential irrigation treatment was initiated, with four different flood-irrigation regimes. Our nomenclature reflects the number and timing of irrigations between harvests: the WET treatment received two irrigations between cuttings; the EARLY treatment was irrigated once, immediately after harvest; the LATE treatment received water midway between cuttings; and the DRY treatment received no supplemental water by irrigation from one harvest until the next. Deficit irrigation treatments were rotated among plots to provide the alfalfa with a recovery period of one complete water cycle between harvest.

Surface Reflectance and Temperature Measurements

Crop canopy reflectances were measured using a Modular Multispectral Radiometer (MMR)¹ with filters simulating the Landsat Thematic Mapper (TM), equipped with 15° field-of-view lenses. Only data from the TM red (0.62–0.69 μm) and NIR (0.78–0.90 μm), and TM thermal (10.42–11.66 μm) will be discussed in this report. The MMR was mounted in a backpack-type yoke and deployed over 1 by 9 m target areas in each plot. The sensor was pointed in a nadir direction, with each lens viewing an area approximately 0.3 m in diameter when the plants were 0.5 m in height.

Multispectral observations were made several times a week at 10:30 MST to coincide with the time of the Landsat overpass. Surface spectral reflectance was calculated as the ratio of radiance measured over each alfalfa target to irradiance measured over a 0.6 by 0.6 m, horizontally positioned, calibrated BaSO₄ reference panel. Correction factors were applied to the BaSO₄ data to compensate for the non-lambertian reflectance properties of the panel. Twelve measurements in each plot were combined to yield an average reflectance and temperature per plot for each band. The entire measurement sequence over 18 experimental plots required about 15 minutes to complete.

Surface temperature data were not corrected for surface emissivity. Because the thermal infrared emissivity of a plant canopy is approximately 0.98, assuming an emissivity of 1.0 resulted in a nearly constant offset of about -1.7°C. Since the precise emissivity of the canopy was unknown, we operationally assumed it to be 1.0. The resulting error should cause a relatively constant bias but should not affect the principles involved.

Agronomic Measurements

Above-ground plant biomass was estimated from four, 0.25 m² circular samples taken several times a week in eight treatment plots over a one-year period from

¹The use of company names and brand names are necessary to report factually on available data; however, the USDA neither guarantees nor warrants the standard of the product, and the use of the name by USDA implies no approval of the product to the exclusion of others that may also be suitable.

20 August 1984 to 5 July 1985. Plants in the field were cut by hand with a curved knife, leaving a stubble height of 2 to 3 cm. Plant material was dried in an oven for at least 48 hrs at 60–70°C. Dry biomass (gm^{-2}) was calculated as the sum of dry weights for the four 0.25 m^2 samples. Plant height was measured along a transect through the center of each plot and averaged to produce an estimate of overall canopy height. Plant materials taken from the biomass samples were used to determine LAI using a Licor Model 3100¹ Leaf Area Meter (LAM).

Meteorologic Measurements

Lysimeters of size 1.0 × 1.0 m by 1.5 m depth were located in three different plots. Throughout the experiment, the lysimeters were irrigated by hand at the same times and with the same amounts of water as the surrounding plots. Weights of the lysimeters were recorded every 30 min during the experiment. A multitude of other meteorologic parameters were monitored every 30 min during the experiment, including air temperature and wind speed (at several heights above the canopy), reflected and incoming solar radiation, PAR, surface and soil temperatures, and vapor pressure. Infrared thermometers (IRT) were situated over each lysimeter to provide 30 min measurements of surface temperature. All meteorologic and radiometric instruments were calibrated periodically during the experiment.

In order to test the above-mentioned hypothesis that r_{ah} is directly related to SR, it was necessary to compute values z_0 and r_{ah} from on-site meteorologic measurements. Values of z_0 were computed using the established linear relation between the measured wind profile data (Brutseart, 1982). According to Eq. (3), z_0 can be determined by extrapolating an observed linear relation between u (at height z) and $\ln(z)$ to the point where $u = 0$ at $z = z_0$. Moran (1990) describes this procedure and the data selection criteria used to assure validity for this data set. Values of r_{ah} were computed based on Eq. (3) with corrections for atmospheric stability suggested by Marht and Ek (1984).

REMOTELY-SENSED ESTIMATION OF AGRONOMIC PARAMETERS

Though the USWCL alfalfa experiment was conducted for two years, this research was limited to periods when spectral data and agronomic measurements were available. For example, biomass and plant height measurements were made two or three times per week from 20 August 1984 to 5 July 1985. LAI was measured twice per week in all treatment plots during one harvest cycle, from June 8 to July 6, 1985. For each of these periods, the meteorologic and spectral data were screened to eliminate obvious problems and equipment failures. For analysis of E, the data was further screened to eliminate days with substantial cloud cover.

These selection criteria resulted in a data set of plant height, biomass, and surface reflectance factors for 183 days over a period of 280 days (from 27 October 1984 to 4 July 1985), encompassing seven harvest periods. LAI data were

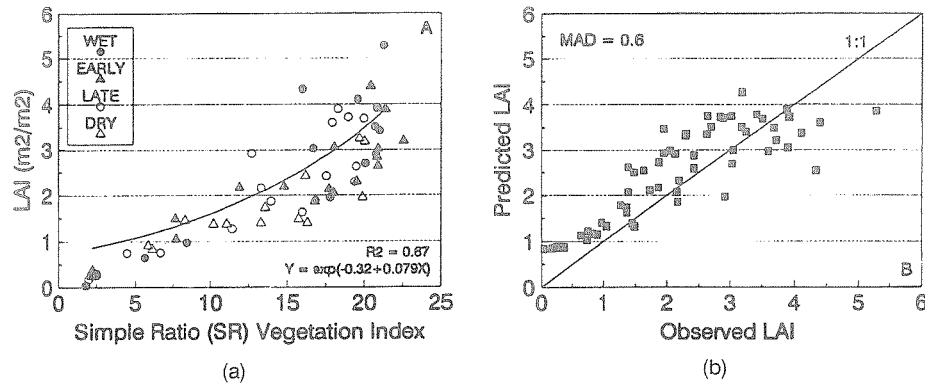


FIGURE 5 (a) Empirical relation between alfalfa leaf area index (LAI) and SR vegetation index for four irrigation treatments ranging from WET to DRY. (b) comparison of observed LAI values with LAI predicted using the relation presented in (a). MAD is the mean absolute difference between the observed and predicted values.

available in the four treatment plots on thirteen days over a 25-day harvest cycle, resulting in a data set of 52 samples. Values of E and corresponding surface temperatures were available for three lysimeters for 80 days from 1 January to 6 January 1985, covering six harvest periods.

LAI

For one harvest cycle, MMR and LAI data were acquired in eight plots for the four different irrigation treatments. The LAI data showed a slightly curvilinear trend with SR (Figure 5(a)). Furthermore, the relation between LAI and SR appeared to be associated with the irrigation treatment (WET, LATE, EARLY or DRY). This was likely due to the change in canopy architecture associated with plant stress. In previous work with this data set, Moran et al. (1990) showed that some spectral vegetation indices were significantly influenced by stress-induced changes in architecture. They concluded that ratioed indices (such as SR) were more likely to minimize the effects of water stress than linear band combinations.

In any case, the relation between SR and LAI over all treatments was significant (0.05 level) and the mean absolute difference (MAD) between observed and predicted values of LAI was 0.6 (Figure 5(b)). It is notable that the SR is less sensitive to changes in LAI when the latter exceeds a value of about 3.0. Thus, the model simulations of LAI would be prone to higher errors for higher LAI values due to the greater uncertainty in remotely-sensed estimates of high LAI values.

Daily Evaporation

Based on T_s and T_a measurements acquired at 1400 hr MST at the three lysimeters, an empirical relation (based on Eq. (4)) was derived for the values E and

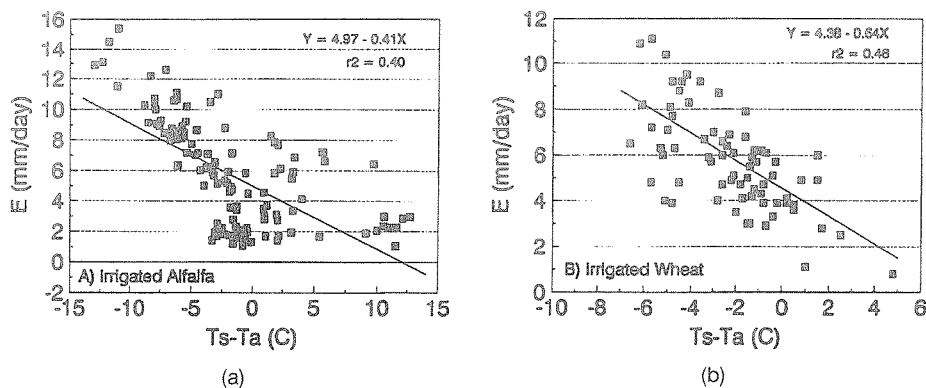


FIGURE 6 (a) Empirical relation between measurements daily surface evaporation (E) from three lysimeters and surface-air temperature ($T_s - T_a$) for irrigated alfalfa. (b) A similar empirical relation for irrigated wheat.

($T_s - T_a$) over a six-month period (Figure 6(a)). The amount of scatter about the regression line ($r^2 = 0.40$) was similar to that found by Jackson et al. (1977) for a similar experiment in irrigated wheat over the limited range of ($T_s - T_a$) from -8 to 5°C (Figure 6(b)). Due to the frequent harvest schedule of the alfalfa crop, a larger range of $T_s - T_a$ and E values were obtained for the alfalfa than for the wheat crop. This larger range emphasized the weakness in the relation originally derived by Jackson et al. (1977) associated with the assumption that $\rho c_p / r_{ah}$ was constant.

Using the on-site measurements of z_0 and r_{ah} with corresponding surface reflectance data, it was possible to (1) confirm the correlation between z_0 and plant height for this data set (Figure 7(a)), (2) evaluate the relation between plant height and spectral vegetation index (Figure 7(b)), and (3) determine an empirical relation between spectral vegetation index and r_{ah} (Figure 7(c)). The relation of plant height and SR was very similar to that of LAI and SR (Figure 5(a)). That is, there appeared to be a curvilinear relation, approaching an asymptote after canopy closure. As in the case of LAI, SR was very sensitive to plant height until canopy closure; then, the amount of scatter increased. Much of the scatter in the relation between r_{ah} and SR could be attributed to variations in wind speed that ranged from $1-4 \text{ ms}^{-1}$ for this data set. The relation between r_{ah} and SR (Figure 7(c)) could be fit by an exponential equation

$$r_{ah} = e^{(4.62 - 0.091\text{SR})}, \quad (9)$$

with r^2 value of 0.86. Based on this relation, it was feasible to use surface reflectance measurements rather than complex meteorologic measurements to evaluate r_{ah} in Eq. (5).

Using Eq. (9) and the data presented in Figure 6(a), the empirical parameters A' and B' of Eq. (5) were evaluated (Figure 8(a)). Results were improved through the use of Eq. (5) rather than Eq. (4) for this analysis; the scatter in the relation was decreased and the r^2 value was increased from 0.40 to 0.50.

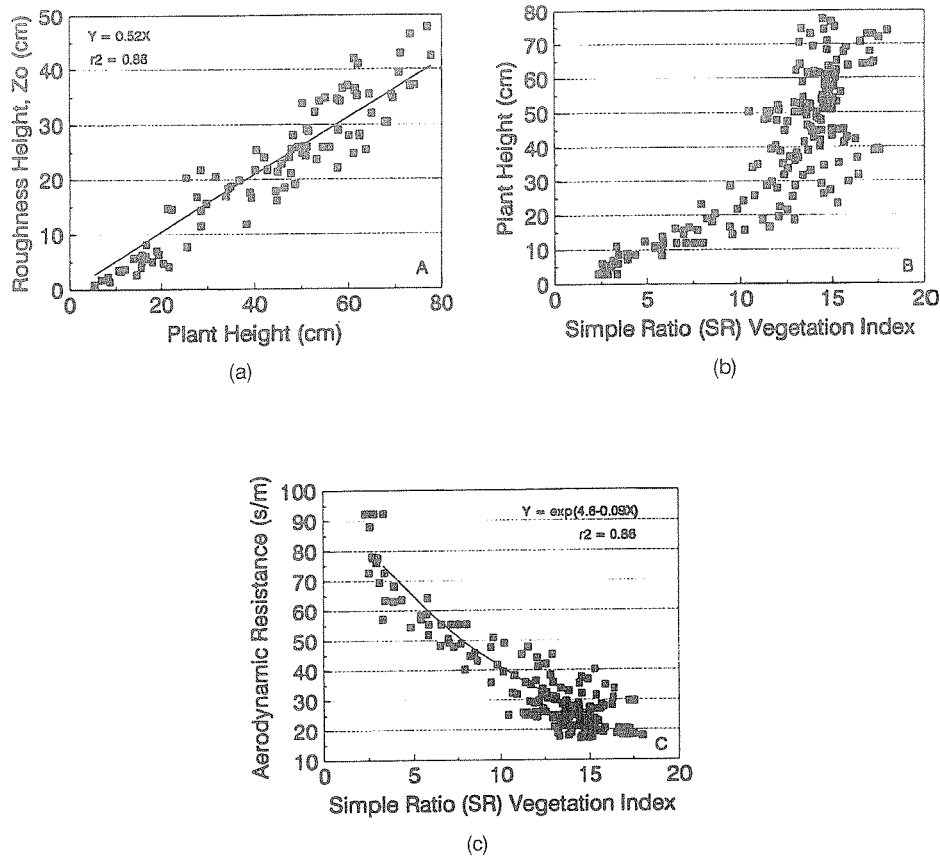


FIGURE 7 (a) Correlation between measurements of aerodynamic roughness height (z_0) and plant height for alfalfa; (b) relation between plant height and the simple ratio (SR) vegetation index; and (c) an empirical relation derived to estimate resistance to heat transfer (r_{ah}) from SR.

However, there was still a great deal of scatter about the regression line and the mean absolute difference (MAD) between predicted E [using Eqs. (5) and (11)] and observed E was 1.9 mm/day (Figure 8(b)).

DEMONSTRATION OF THE MODEL

A demonstration of the model was conducted to evaluate its performance using data obtained from one alfalfa field plot over the period from day 159 to day 189 in 1985. Alfalfa in this plot was cut on day 157 and the plot was irrigated on day 158. The plot received 15.6 mm of water by this irrigation, while the lysimeter in the plot received 12.9 mm of water. The plot and lysimeter did not receive any additional water during this growth period. Canopy height, vegetation biomass and LAI were measured approximately every 4 days during the growth period.

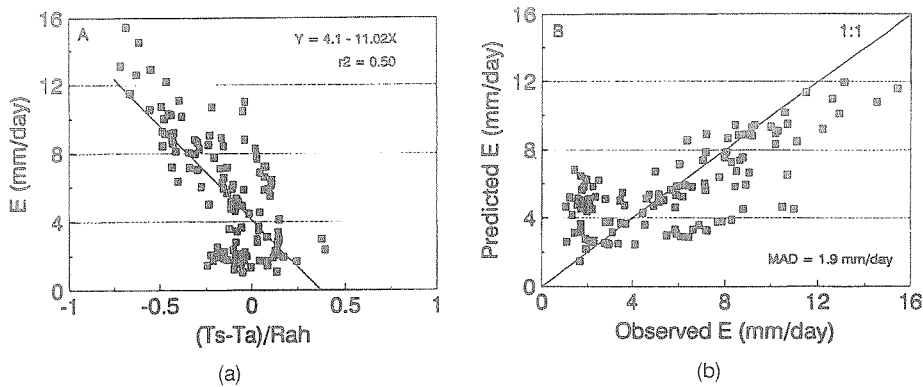


FIGURE 8 (a) Empirical relation between observed daily surface evaporation (E) from three lysimeters and surface-air temperature ($T_s - T_a$) divided by the resistance to heat transfer (r_{ah}) for irrigated alfalfa. The r_{ah} values were estimated based on the simple ratio (SR) vegetation index and Eq. (9). (b) Comparison of measured daily evaporation values (E) with E values predicted using Eqs. (5) and (9) and measurements surface and air temperature and surface reflectance. MAD is the mean absolute difference between the observed and predicted values.

The demonstration was conducted in two steps. First, field observations of LAI and E were used to calibrate the model rather than remotely-sensed observations to insure that any differences between modeled and observed conditions were not due to inaccuracies in estimating LAI and E from remotely-sensed data. Second, the vegetation growth submodel and the soil water balance submodel were run using periodic remotely-sensed estimates of LAI and E for model calibration.

Model Results with Field Observations

In this run, all available field observations were used in calibrating the model to see if the natural detail in the data could be reproduced by the simple model. Certain model parameters [specific leaf area, extinction coefficient and the energy conversion efficiency in Eq. (8)] were determined directly from growth analysis of the field data.

Results from the vegetation growth submodel are presented in Figure 9(a). In most cases, the LAI simulation fit the corresponding observations, except there was a tendency for the submodel to overestimate LAI early in the growth period. The change in slope of the LAI simulation at day 174 coincided with the observed onset of flowering in the crop. Simulated biomass increased over the duration of the growth period and was in good agreement with the observations, except for the tendency for the submodel to overestimate biomass early in the growth period.

Results from the soil water balance submodel are presented in Figure 9(b). The general trend in daily E over the growth period was simulated well. The increase in daily E before day 168 resulted from the increase in the vegetation canopy over this period. This effect is illustrated by the steady increase in the value of F_{GC}

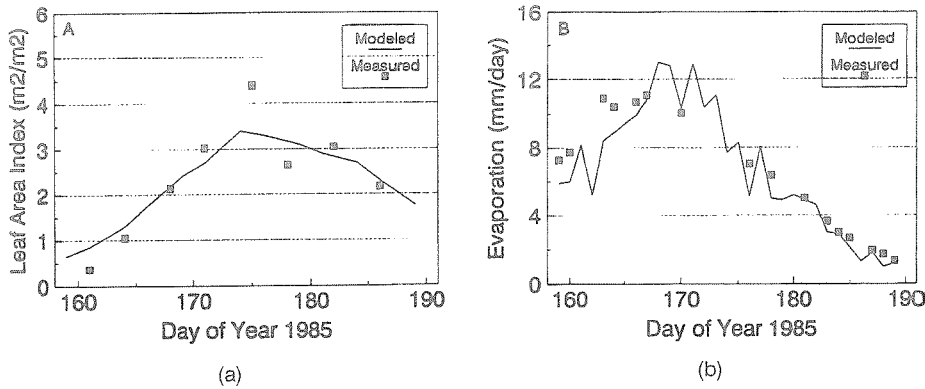


FIGURE 9 Demonstration of the (a) vegetation growth submodel and (b) soil water balance submodel based on periodic field observations of alfalfa canopy leaf area index and daily evapotranspiration, respectively.

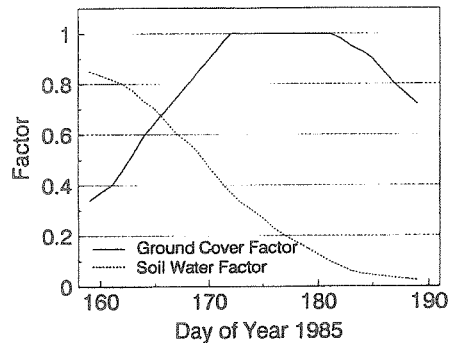


FIGURE 10 Computed daily values of the two factors (F_{sw} and F_{GC}) that determine E from E_p in the model.

over the first half of the growth period (Figure 10). Data presented in Figure 10 also showed a steady decrease in the value of F_{sw} as a result of the decrease in soil moisture over the growth period shown in Figure 9(b). This decline in soil moisture resulted in the decrease in simulated daily E after day 171, when the value of F_{GC} was at or near 1. Based on model constraints, a drop in the soil moisture below 30% of field capacity would result in a decrease in simulated daily E . However, the underestimation of modeled E prior to day 168 suggests that the assumption of zero evaporation over bare soil may not be correct.

Model Results with Remotely-Sensed Estimations

In this run, periodic remotely-sensed estimates of LAI and E were used for model calibration. This run differs from that conducted in the previous section. The simulation results presented in Figure 9 were based on calibration with the

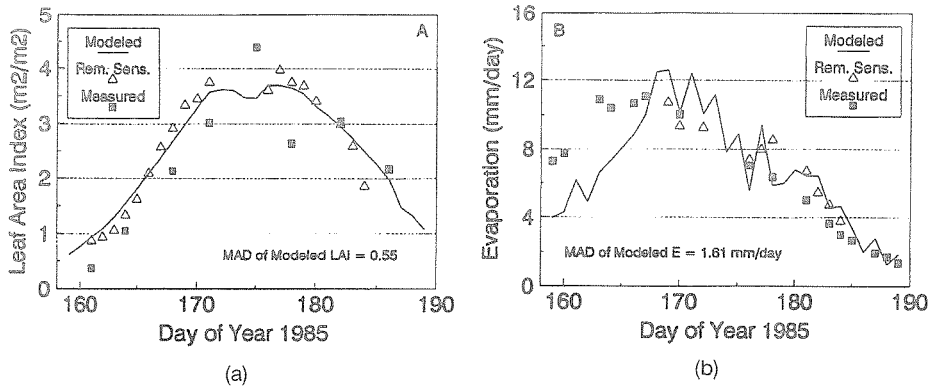


FIGURE 11 Modeled (a) canopy leaf area index and (b) daily evapotranspiration (E) based on the vegetation and soil submodels with periodic remotely-sensed estimates of LAI and E, respectively. Field observations of LAI and E were included for comparison with simulated and remotely-sensed estimates. MAD is the mean absolute difference between the observed and modeled values.

field observations and then compared to the same field observations. The simulation in this section was based only on meteorological data and periodic remotely-sensed estimates of LAI and E. Then, the results were compared with the field observations of LAI and E for a more independent validation.

The LAI simulation based on remotely-sensed estimates (Figure 11(a)) differed slightly from the simulation based on field observations (Figure 9(a)). However, in both cases, the simulated values corresponded well with field observations. The deviation between simulated and observed values of LAI in Figure 11(a) was partly due to the error associated with using remotely-sensed data for periodic estimations of LAI. It was notable that the MAD of observed LAI and that predicted using remote sensing techniques (Figure 5(b)) was equal to the MAD of observed and model-simulated LAI (Figure 11(a)).

In general, daily E values simulated with the model and periodic remotely-sensed estimates of E corresponded well with field observations (Figure 11(b)). The data in Figure 11(b) illustrate an inherent feature of this combined modeling/remote sensing approach for simulating daily E. That is, the simple model works best when periodic inputs are evenly scattered throughout the regrowth period from cutting to senescence or harvest. In this model demonstration (Figure 11(b)), the errors in daily E were largest for the 10-day period from day 159 to day 169 during which there were no remotely-sensed data. During this period, the simulated trend compared well with field observations but the absolute values were lower than the field observations by up to 4 mm/day. When more observations were available (as in the calibration presented in Figure 9(b)), the model simulation was greatly improved. Based on limited remotely-sensed data, the model resulted in a MAD of simulated and observed values of 1.61 mm/day over a range of E values from 1 to 12 mm/day. This MAD was lower than the MAD computed for the estimation of E using only the remotely-sensed data (where MAD = 1.9 mm/day).

CONCLUDING REMARKS

As stated in the introduction, the intent of this work was not to develop best methods for estimation of model inputs (LAI and E) from remotely-sensed surface reflectance factors and temperature. Rather, the intent was to use existing methods for estimation of LAI and E with sufficient accuracy for demonstrating this combined modeling/remote sensing approach. Thus, the empirical and semi-empirical relations used here were appropriate for this analysis but could lead to limitations at local and regional scales due to the site- and crop-specific nature of the derived relations. Further work in remote sensing should be directed towards operational, regional approaches based on a more physically-based strategy. On the other hand, if the model were to be applied to the same crop type in the same location year after year, the semi-empirical relations between remotely-sensed data and LAI and E developed during the first year could be used for simulations in subsequent years.

The model formulation appeared to be adequate for simulating the evapotranspiration and biomass growth in this demonstration involving alfalfa grown in an arid environment. We anticipate the best performance from this type of model in arid and semi-arid climates, where the evaporative demand of the atmosphere is large, rainfall events are infrequent and the soil surface is usually dry. A second demonstration of the model was conducted for the Walnut Gulch semi-arid rangeland watershed in southeastern Arizona (Maas et al., 1993). Based on the results presented here and results for the rangeland site, it appears that one remotely-sensed observation per week would be sufficient for simulation of a rapidly-growing, agricultural crop and one observation per month may suffice for the rangeland site.

Additional tests must be performed to evaluate the performance of the model under different soil water and vegetation cover conditions. The effect of the frequency of remotely-sensed LAI and E data on model accuracy must also be investigated. Should the results of these tests be favorable, this combined modeling/remote sensing approach could become a valuable tool for resource managers in conducting operational, near real-time monitoring of regional water and biomass resources. Since the meteorologic and remotely-sensed information used in the model has a spatial dimension, the model could easily be incorporated into a Geographical Information System (GIS) to facilitate regional resource monitoring, assessment and forecasting.

ACKNOWLEDGMENTS

We are indebted to many scientists and technicians at the U.S. Water Conservation Laboratory who assisted in the acquisition of the massive data set used in this analysis, especially Ray Jackson, Tom Clarke, Bob Reginato, Kurt Clawson, Stephanie Johnson, Harold Kelly and Ron Seay. Terry Mills put in extraordinary effort to safely archive and retrieve these data. And we are particularly grateful to David Shannon for writing the flexible program that allowed us to auto-

matically compile this data subset from the many hundreds of individual data files.

References

- Brown, K. W. (1969) A model of the photosynthesizing leaf. *Physiologia Plantarum* 22: 620–637.
- Brutseart, W. H. (1982) *Evaporation into the Atmosphere*, D. Reidel Publ. Co., London, England, 299 p.
- Charles-Edwards, D. A., Doley, D. and Rimmington, G. M. (1986) *Modeling Plant Growth and Development*, Academic Press, Orlando, FL, 235 p.
- Clothier, B. E., Clawson, K. L., Pinter, P. J., Jr., Moran, M. S., Reginato, R. J. and Jackson, R. D. (1986) Estimation of soil heat flux from net radiation during the growth of alfalfa. *Agriculture and Forest Meteorology* 37: 319–329.
- Jackson, R. D. (1985) Evaluating evapotranspiration at local and regional scales. *Proc. IEEE* 73: 1086–1096.
- Jackson, R. D. and Huete, A. R. (1992) Interpreting vegetation indices. *Preventative Veterinary Medicine* 11: 185–200.
- Jackson, R. D., Reginato, R. J. and Idso, S. B. (1977) Wheat canopy temperature: A practical tool for evaluating water requirements. *Water Resources Research* 13: 651–656.
- Jackson, R. D., Slater, P. N. and Pinter, P. J., Jr. (1983) Discrimination of growth and water stress in wheat by various vegetation indices through clear and turbid atmospheres. *Rem. Sens. Environ.* 13: 187–208.
- Maas, S. J. (1988a) Use of remotely-sensed information in agricultural crop growth models. *Ecological Modelling* 41: 247–268.
- Maas, S. J. (1988b) Using satellite data to improve model estimates of crop yield. *Agronomy Journal* 80: 655–662.
- Maas, S. J. (1991a) Validation of GRAMI wheat yield estimates for North Dakota using Landsat MSS data. *Preprints, 20th Conference on Agricultural and Forest Meteorology*, 10–13 Sept. 1991, Salt Lake City, UT, Amer. Meteorol. Soc., 228–231.
- Maas, S. J. (1991b) Use of remotely-sensed information in plant growth simulation models. *Advances in Agronomy* (Council for Scientific Research Integration, Trivandrum, India), 1: 17–26.
- Maas, S. J. (1992) *GRAMI: A Crop Growth Model That Can Use Remotely-Sensed Information*, ARS-91, U.S. Dept. of Agric., Washington, DC, 78 p.
- Maas, S. J. (1993a) Parameterized model of gramineous crop growth: I. Leaf area and dry mass simulation. *Agronomy Journal* 85: 348–353.
- Maas, S. J. (1993b) Parameterized model of gramineous crop growth: II. Within-season simulation calibration. *Agronomy Journal* 85: 354–358.
- Maas, S. J., Jackson, R. D., Idso, S. B., Pinter, P. J., Jr. and Reginato, R. J. (1989) Incorporation of remote-sensed indicators of water stress in a crop growth simulation model. *Preprints, 19th Conference on Agricultural and Forest Meteorology*, 7–10 March 1989, Charleston, SC, Americal Meteorological Society, Boston, MA, 228–231.
- Maas, S. J., Moran, M. S. and Jackson, R. D. (1992) Combining remote sensing and modeling for regional resource monitoring, Part II: A simple model for estimating surface evaporation and biomass production. *Proc. ASPRS/ACSM/RT92*, Washington, DC, 3–7 August 1992, 225–234.
- Maas, S. J., Moran, M. S., Weltz, M. A. and Blanford, J. (1993) Model for simulating surface evaporation and biomass production utilizing routine meteorological and remotely-sensed data. *Proc. 1993 ASPRS Ann. Meeting*, 15–19 Feb., New Orleans, LA.
- Mahrt, L. and Ek, M. (1984) The influence of atmospheric stability on potential evaporation. *J. Climate and Appl. Meteorol.* 23: 222–234.
- Meyer, W. S. and Green, G. C. (1980) Water use by wheat and plant indicators of available soil water. *Agronomy Journal* 72: 253–257.
- Monteith, J. L. (1973) *Principles of Environmental Physics*, Elsevier Press, New York, 241 pp.
- Moran, M. S. (1990) A satellite-based approach for evaluation of the spatial distribution of evapotranspiration from agricultural lands. *Ph.D. Diss.*, University of Arizona, Tucson, AZ, 223 pp.
- Moran, M. S. and Jackson, R. D. (1991) Assessing the spatial distribution of evapotranspiration using remotely-sensed inputs. *J. of Env. Quality* 20: 725–737.
- Moran, M. S., Maas, S. J. and Jackson, R. D. (1992) Combining remote sensing and modeling for regional resource monitoring, Part II: A simple model for estimating surface evaporation and biomass production. *Proc. ASPRS/ACSM/RT92*, Washington, DC, 3–7 August 1992, 215–224.

- Moran, M. S., Pinter, P. J., Jr., Allen, S. A. and Clothier, B. E. (1990) Effect of water stress on the canopy architecture and spectral indices of irrigated alfalfa. *Rem. Sens. of Environ.* 29: 251-261.
- Pinter, P. J., Jr., Kelly, H. L., Jr. and Schnell, S. (1987) Spectral estimation of alfalfa biomass under conditions of variable cloud cover. *Proc. of 18th Conf. Agric. and For. Meteorol. and 8th Conf. on Biometeorol.*, 15-18 September, West Lafayette, IN, 83-86.
- Ritchie, J. T. and Burnett, E. (1971) Dryland evaporative flux in a subhumid climate: II. Plant influences. *Agronomy Journal* 63: 56-62.
- Ranson, K. J. and Daughtry, C. S. T. (1987) Scene shadow effects on multispectral response. *IEEE Trans. on Geosci. and Rem. Sens.* GE-25: 502-509.
- Rosenthal, W. D., Arkin, G. F., Shouse, P. J. and Jordan, W. R. (1987) Water deficit effects on transpiration and leaf growth. *Agronomy Journal* 79: 1019-1026.
- Sellers, P. J., Mintz, Y., Sud, Y. C. and Dalcher, A. (1986) A simple biosphere model (SiB) for use within general circulation models. *J. of Atm. Sci.* 43: 505-531.
- Tucker, C. J. (1979) Red and photographic infrared linear combinations for monitoring vegetation. *Rem. Sens. of Environ.* 8: 127-150.
- Van Bavel, C. H. M. (1966) Potential evaporation: The combination concept and its experimental verification. *Water Resources Research* 2: 455-467.